1-2017

# PTPRO represses ERBB2-driven breast oncogenesis by dephosphorylation and endosomal internalization of ERBB2.

H Dong

L Ma

J Gan

W Lin

Rakesh Kumar
*George Washington University*

***See next page for additional authors***

OPEN

Oncogene (2016), 1–13

www.nature.com/onc

ORIGINAL ARTICLE

# PTPRO represses ERBB2-driven breast oncogenesis by dephosphorylation and endosomal internalization of ERBB2

H Dong[1,9], L Ma[2,9], J Gan[1], W Lin[1], C Chen[1], Z Yao[1], L Du[1], L Zheng[1], C Ke[1], X Huang[3], H Song[4], R Kumar[5], SC Yeung[1,6,7] and H Zhang[1,8]

The plasma membrane-associated tyrosine phosphatase PTPRO is frequently transcriptionally repressed in cancers and signifies poor prognosis of breast cancer patients. In this study, deletion of *Ptpro* in *MMTV-Erbb2* transgenic mice dramatically shortened the mammary tumor latency and accelerated tumor growth due to loss of *Ptpro* within the breast cancer cells but not in surrounding tissue as confirmed by hetero-transplantation studies. Both *in vitro* and *in vivo* data demonstrated that the phosphatase activity was required for the inactivation of ERBB2 and its downstream signaling. PTPRO regulated the phosphorylation status of ERBB2 at Y1248. Co-immunoprecipitation and proximity ligation assay (Duolink) indicated that PTPRO directly physically interacted with ERBB2. Moreover, PTPRO phosphatase activity shortened the half-life of ERBB2 by increasing endocytotic degradation. PTPRO reexpression by demethylation treatment using 5-azacytidine reduced the proliferation and colony formation potential in ERBB2-positive breast cancer cells. Taken together, PTPRO inhibited ERBB2-driven breast cancer through dephosphorylation leading to dual effects of ERBB2 signaling suppression and endosomal internalization of ERBB2, Therefore, reexpression of PTPRO may be a potential therapy for ERBB2-overexpressing breast cancer.

*Oncogene* advance online publication, 27 June 2016; doi:10.1038/onc.2016.213

## INTRODUCTION

Dysregulation of the epidermal growth factor receptors (EGFRs; that is, type I receptor tyrosine kinases (RTKs): ERBB1 (EGFR), ERBB2 (HER2), ERBB3 and ERBB4) drives the development and progression of a wide range of cancers.[1] Recently, transcriptome-wide array-based analyses have been used to classify human breast cancer into four main molecular types: luminal A, luminal B, ERBB2-enriched and basal-like.[1] ERBB2-enriched breast cancers with *ERBB2* amplification account for approximately a quarter of all breast cancer and is associated with poor prognosis.[1–4] Despite the clinical benefits resulted from ERBB2-targeted therapeutics, a substantial percentage of ERBB2-overexpressing cancer fail to respond or develop secondary resistance to the current targeted treatments.[2–4] Thus, for a complete understanding of ERBB2 functions, it is critical to identify the novel mechanistic control of ERBB2 signaling, which will advance the intervention and diagnosis for ERBB2-positive cancers.

Reversible phosphorylation of a specific tyrosine residue is governed by the balanced action of PTKs and protein tyrosine phosphatases (PTPs). Specifically in ERBB2-overexpressing breast cancer, ERBB2 dimerization initiates phosphorylation on tyrosine residues in the cytoplasmic tail of ERBB2,[5,6] resulting in activation of downstream signaling that drives tumor growth.[7] Dysregulation of PTPs has been recognized as an important cause of cancers.[8–10] PTP receptor type O (PTPRO, also known as GLEPP1) is a member of the transmembrane receptor family of PTPs that is phylogenetically on a branch of the tyrosine phosphatome distinct from other PTPs.[11–17] Besides its functions in embryonic development, immune response and neuron differentiation,[18,19] PTPRO has been assumed to act as a putative tumor suppressor in several cancer types.[20–23] We recently presented evidence that the DNA methylation status of *PTPRO* is a prognostic factor in ERBB2-positive breast cancer.[24] However, the inherent role of PTPRO in oncogenesis has not been established in physiologically relevant whole animal models. The current knowledge gaps also include the following: the specific tyrosine residue of ERBB2 that is selectively dephosphorylated by PTPRO is unknown; the mechanism by which PTPRO inhibits ERBB2-driven tumorigenesis remains largely unknown; the potential of PTPRO as a therapeutic target in breast cancer has not been evaluated.

In this study, we investigated these unknown questions, and discovered that the loss of *Ptpro* resulted in amplified ERBB2 oncogenic signaling, feeding into cancerous phenotypes in genetic models and ERBB2-overexpressing human breast tumors. Meanwhile, we discovered the novel mechanisms responsible for tumor suppression by PTPRO, which involved dephosphorylation leading to not only blockade of ERBB2 signaling but also endocytotic degradation. Further, we revealed the therapeutic potential of reexpression of PTPRO by demethylation treatment.

[1]Cancer Research Center, Shantou University Medical College, Shantou, China; [2]Department of Gastroenterology, University of Texas MD Anderson Cancer Center, Houston, TX, USA; [3]MOE Key Laboratory of Model Animal for Disease Study, Model Animal Research Center of Nanjing University, Nanjing, China; [4]Department of Cell Biology, Xi'an Jiaotong University Suzhou Academy, Suzhou, China; [5]Department of Biochemistry and Molecular Medicine, School of Medicine and Health Sciences, George Washington University, Washington DC, USA; [6]Department of Emergency Medicine, University of Texas MD Anderson Cancer Center, Houston, TX, USA; [7]Department of Endocrine Neoplasia and Hormonal Disorders, University of Texas MD Anderson Cancer Center, Houston, TX, USA and [8]Department of Biotherapy, Affiliated Cancer Hospital of Shantou University Medical College, Shantou, China. Correspondence: Professor H Zhang, Cancer Research Center, Shantou University Medical College, Xinling Road No. 22, Shantou 515041, China or Professor SC Yeung, Department of Endocrine Neoplasia and Hormonal Disorders, University of Texas MD Anderson Cancer Center, 1515 Holcombe Boulevard, Houston, TX 77030, USA. E-mail: haozhang@stu.edu.cn or syeung@mdanderson.org

[9]These authors contributed equally to this work.

Received 12 November 2015; revised 5 May 2016; accepted 8 May 2016

## RESULTS

### *Ptpro* deletion enhanced mammary tumorigenesis in *MMTV-Erbb2* transgenic mice

The major knowledge gap about the role of *Ptpro* in carcinogenesis is the lack of *in vivo* evidence. To validate the tumor-suppressor role of PTPRO, we examined the influence of *Ptpro* knockout ($Ptpro^{-/-}$) on *MMTV-Erbb2*-driven mammary tumorigenesis in mice. To minimize the variability of tumor formation due to strain difference and heterogeneity of genetic background, we first obtained the $Ptpro^{-/-}$ genotype in a near-pure FVB/N genetic background (99.90% FVB/N) by backcrossing $Ptpro^{-/-}$ mice to FVB/N mice for 10 generations (see the Methods for details). No spontaneous mammary tumors were observed in 30 virgin $Ptpro^{-/-}$ female mice and 32 $Ptpro^{-/-}$ breeding dames with multiple pregnancies after follow-up periods of up to 2 years. This suggested that loss of *Ptpro* alone might not be sufficient to induce breast tumorigenesis. We investigated the influence of deleting *Ptpro* on *Erbb2*-driven mammary gland tumorigenesis by crossing *MMTV-Erbb2* mice (100% FVB/N) with $Ptpro^{-/-}$ mice (99.90% FVB/N). We compared breast tumorigenesis in $Ptpro^{-/-}$/*MMTV-Erbb2* with $Ptpro^{+/+}$/*MMTV-Erbb2* mice. In a longitudinal study, palpable mammary tumors were detected between 26 and 49 weeks of age in 35 $Ptpro^{+/+}$/*MMTV-Erbb2* virgin female mice (one mouse was lost soon after genotyping); in contrast, palpable tumors were detected in 36 $Ptpro^{-/-}$/*MMTV-Erbb2* virgin female mice between 17 and 34 weeks of age (Figure 1a). The median time to detection of breast tumors was significantly shorter in $Ptpro^{-/-}$/*MMTV-Erbb2* compared with $Ptpro^{+/+}$/*MMTV-Erbb2* (median: 27 weeks vs 36 weeks, respectively; $P < 0.001$, log rank test). All the mice were killed at 9 weeks after tumor detection. The dissected index tumors in $Ptpro^{-/-}$/*MMTV-Erbb2* mice weighed significantly more than those in $Ptpro^{+/+}$/*MMTV-Erbb2* mice at the same time point after tumor detection ($P = 0.017$; Figure 1b and Supplementary Figure 1A). To compare the rate of tumor progression, we measured the tumor sizes for 9 weeks since detection. Tumor volumes from week 5 to week 9 in the $Ptpro^{-/-}$/*MMTV-Erbb2* group were significantly larger than the corresponding volumes in the $Ptpro^{+/+}$/*MMTV-Erbb2* group (Figure 1c). We also documented the number of tumors at 9 weeks after the first tumor was detected. Together, deletion of *Ptpro* remarkably accelerated *Erbb2*-driven mammary tumorigenesis, validating the long suspected tumor-suppressor activity of *Ptpro* in a whole animal model of breast cancer for the first time.

Cell proliferation, as judged by IHC for phospho-S10-histone H3 (phos-H3) and PCNA in sections of dissected tissues, was significantly enhanced in $Ptpro^{-/-}$/*MMTV-Erbb2* vs $Ptpro^{+/+}$/*MMTV-Erbb2* mice (12% vs 6% phos-H3-positive cells, and 23% vs 9% PCNA-positive cells, respectively; $P < 0.001$ for both; Figure 1d). However, there was no statistically significant difference in the level of apoptosis between the two genotypes (Figure 1d). Thus, genetic deletion of *Ptpro* accelerated the growth rate of *Erbb2*-driven mammary tumors primarily through stimulating cell proliferation.

In a cross-sectional study of 24-week-old mice of these two genotypes (five mice per group), whole-mount analysis revealed a lower degree of mammary epithelial hyperplasia in $Ptpro^{+/+}$/*MMTV-Erbb2* glands as compared with $Ptpro^{-/-}$/*MMTV-Erbb2* (Figure 1e). We also noticed more mitotic cells in $Ptpro^{-/-}$/*MMTV-Erbb2* tumors as compared with $Ptpro^{+/+}$/*MMTV-Erbb2* tumors in 32-week-old mice (Supplementary Figure 1B). In brief, prevalence of advanced lesions and tumors in $Ptpro^{-/-}$/*MMTV-Erbb2* mice were consistent with the accelerated tumorigenesis due to *Ptpro* deletion.

To investigate whether the observed accelerated breast tumorigenesis in $Ptpro^{-/-}$/*MMTV-Erbb2* mice was primarily due to loss of *Ptpro* within the mammary tumor or a consequence of possible off-target effects on systemic circulating factors or non-cancerous host tissues, we transplanted mammary epithelial tissues from both genotypes of *Erbb2* transgenic mice when 30 weeks of age. One million primary cells from two genotypic mouse tumors were implanted under the dorsal skin of female nude mice at the right and left flanks, respectively. $Ptpro^{-/-}$/*MMTV-Erbb2* breast cells developed into palpable tumors faster than the $Ptpro^{+/+}$/*MMTV-Erbb2* implanted in the same mouse after implantation ($P = 0.043$, two-sided paired *t*-test; Figure 1f). The excised $Ptpro^{-/-}$/*MMTV-Erbb2* tumors were significantly heavier than the $Ptpro^{+/+}$/*MMTV-Erbb2* tumors when the mice were killed at 6 weeks after tumor appearance ($P = 0.047$, two-sided paired *t*-test; Figure 1g). These results indicated that the accelerated mammary tumor development in $Ptpro^{-/-}$/*MMTV-Erbb2* mice was not an off-target consequence due to loss of *Ptpro* in the whole mouse. Collectively, these *in vivo* data demonstrated that loss of *Ptpro* in mammary epithelium caused acceleration of *Erbb2*-driven breast carcinogenesis and progression.

### PTPRO selectively dephosphorylated ERBB2 at Y1248

Although it is known PTPRO can dephosphorylate ERBB2,[25] the specific tyrosine residue of ERBB2 that is selectively dephosphorylated by PTPRO is unknown. We thus performed co-immunoprecipitation studies using the SKBR3 cell line transfected with empty vector or *PTPRO* vector with or without heregulin to stimulate ERBB2 signaling. Precipitated proteins were separated by SDS–polyacrylamide gel electrophoresis followed by immunoblotting with anti-PTPRO, anti-p-ERBB2 (Y877), anti-p-ERBB2 (Y1112), anti-p-ERBB2 (Y1139), anti-p-ERBB2 (Y1196), anti-p-ERBB2 (Y1221) or anti-p-ERBB2 (Y1248) and anti-ERBB2 antibodies (Figure 2a). The ERBB2 associated with immunoprecipitated PTPRO had detectable phosphorylation at several phosphorylation sites but not at Y1248. These data identified that PTPRO dephosphorylated ERBB2 at Y1248.

Further, we used proximity ligation assay[26] to detect whether there is a direct intermolecular interaction between PTPRO and ERBB2. SKBR3 cells were fixed and incubated with anti-ERBB2 and anti-PTPRO antibodies, followed by Duolink reaction. The results showed that PTPRO and ERBB2 directly interacted at the cell membrane and in the cytoplasm of cancer cells, while knocking down either PTPRO or ERBB2 abolished the interaction (Figure 2b). Together, we for the first time identified the specific tyrosine site of ERBB2 dephosphorylated by PTPRO and the subcellular locations where direct interaction between PPTRO and ERBB2 occurs.

### Loss of PTPRO phosphatase activity mimicked *PTPRO* deletion, leading to increased tumor cell growth

We next examined the cellular mechanisms by which deletion of *Ptpro* enhanced *Erbb2*-dependent growth and tumorigenesis. To investigate whether the PTPRO could regulate ERBB2 cellular activities at endogenous expression level, we generated mouse embryonic fibroblasts (MEFs) derived from two genotypic mice and stably transfected them with plasmid FUGW-*Erbb2* (Figure 3a). The growth rate was significantly higher in *Erbb2*/$Ptpro^{-/-}$ MEFs than in *Erbb2*/$Ptpro^{+/+}$ MEFs at 48 h ($P = 0.025$) and 72 h ($P = 0.002$; Figure 3b). Further, *Erbb2*/$Ptpro^{-/-}$ MEFs also showed increased colony formation compared with *Erbb2*/$Ptpro^{+/+}$MEFs ($P = 0.005$; Figure 3c). Flow cytometry assay revealed that the percentage of cells in the G1 phase decreased to the much lower level in *Erbb2*/$Ptpro^{-/-}$ MEFs and this was accompanied by a concomitant increase of accumulated cells in the S phase (Figure 3d), thus indicating blocked cell cycle by PTPRO expression. Meanwhile, Annexin-V-fluorescein isothiocyanate (FITC) and propidium iodide (PI) dual staining assay did not show any difference in apoptosis between the *Erbb2*/$Ptpro^{+/+}$ and *Erbb2*/$Ptpro^{-/-}$ MEFs (Figure 3e).

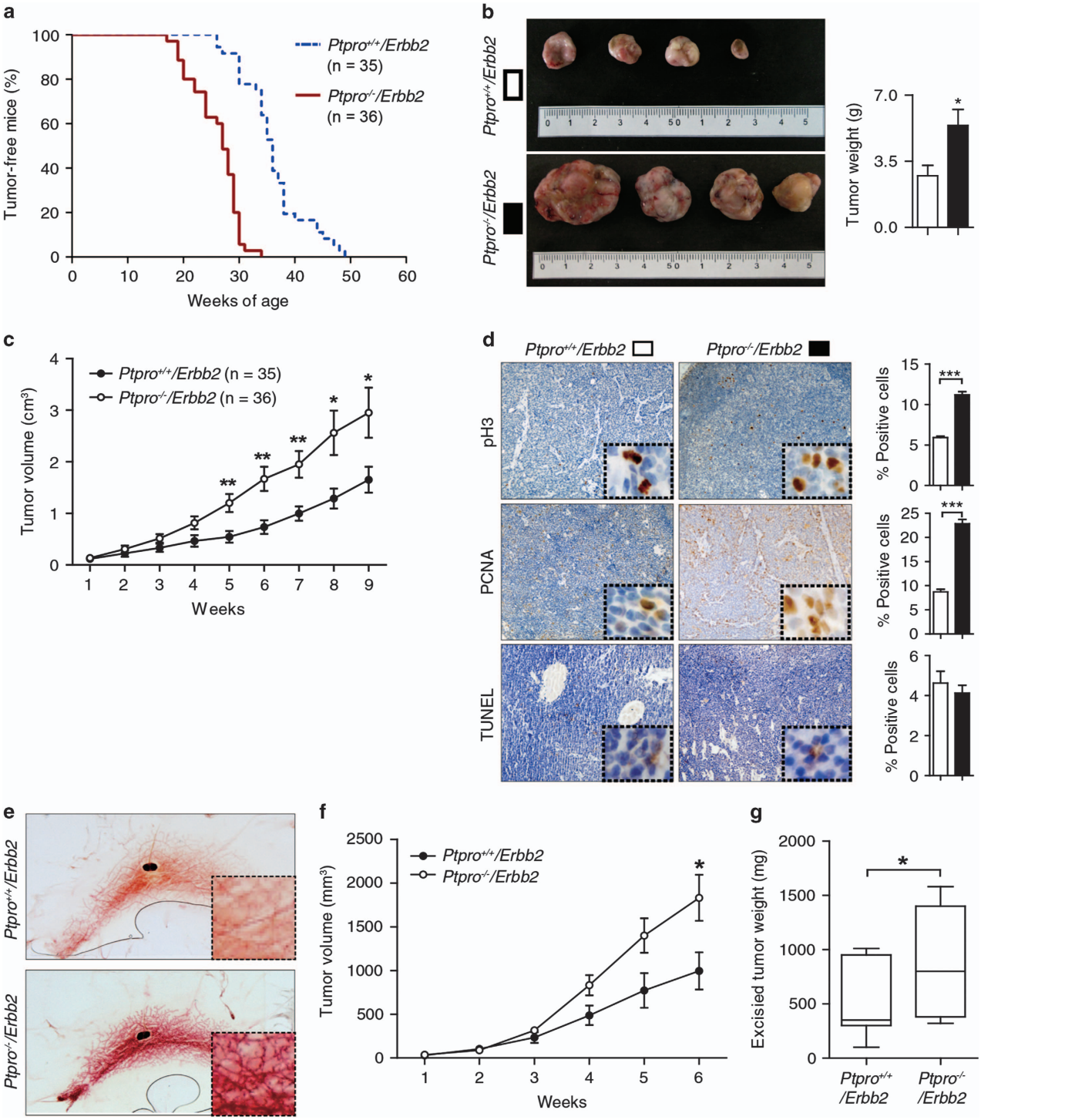


**Figure 1.** *Ptpro* deficiency facilitated *MMTV-Erbb2*-induced mammary tumorigenesis. (**a**) Kaplan–Meier plots of tumor-free survival in *Ptpro*$^{+/+}$*/MMTV-Erbb2* and *Ptpro*$^{-/-}$*/MMTV-Erbb2* mice. (**b**) Representative images of tumors from all of the *Ptpro*$^{-/-}$*/MMTV-Erbb2* mice and littermate control (left). Harvested tumor weights were determined (right). (**c**) Tumor volumes were measured at the indicated weeks. (**d**) Representative images of immunohistochemistry detection of pH3 and PCNA, and TUNEL in mouse tumors of *Ptpro*$^{-/-}$*/MMTV-Erbb2* and littermate control (left). Bar charts represent the quantification of staining (right). Samples shown are representative of three independent experiments ($n = 5$ per genotype). Error bars indicate s.e.m. *$P < 0.05$, **$P < 0.01$, ***$P < 0.001$ by Student's *t*-test. (**e**) Whole-mount mammary gland preparations (24 W) revealed hyperplasia in *Ptpro*$^{-/-}$*/MMTV-Erbb2* glands compared with littermate controls. The bottom panels showed a *Ptpro*$^{-/-}$*/MMTV-Erbb2* gland with pervasive epithelial hyperplasia. (**f**) Average tumor volume was calculated after initiation of palpable tumors. Error bars indicate s.e.m. ($n = 6$ in *Ptpro*$^{-/-}$*/MMTV-Erbb2*, and 6 in *Ptpro*$^{+/+}$*/MMTV-Erbb2*). *$P = 0.043$, two-sided paired *t*-test. (**g**) The box plots of the weights of tumors harvested at 6 weeks are shown. *$P = 0.047$, two-sided paired *t*-test.

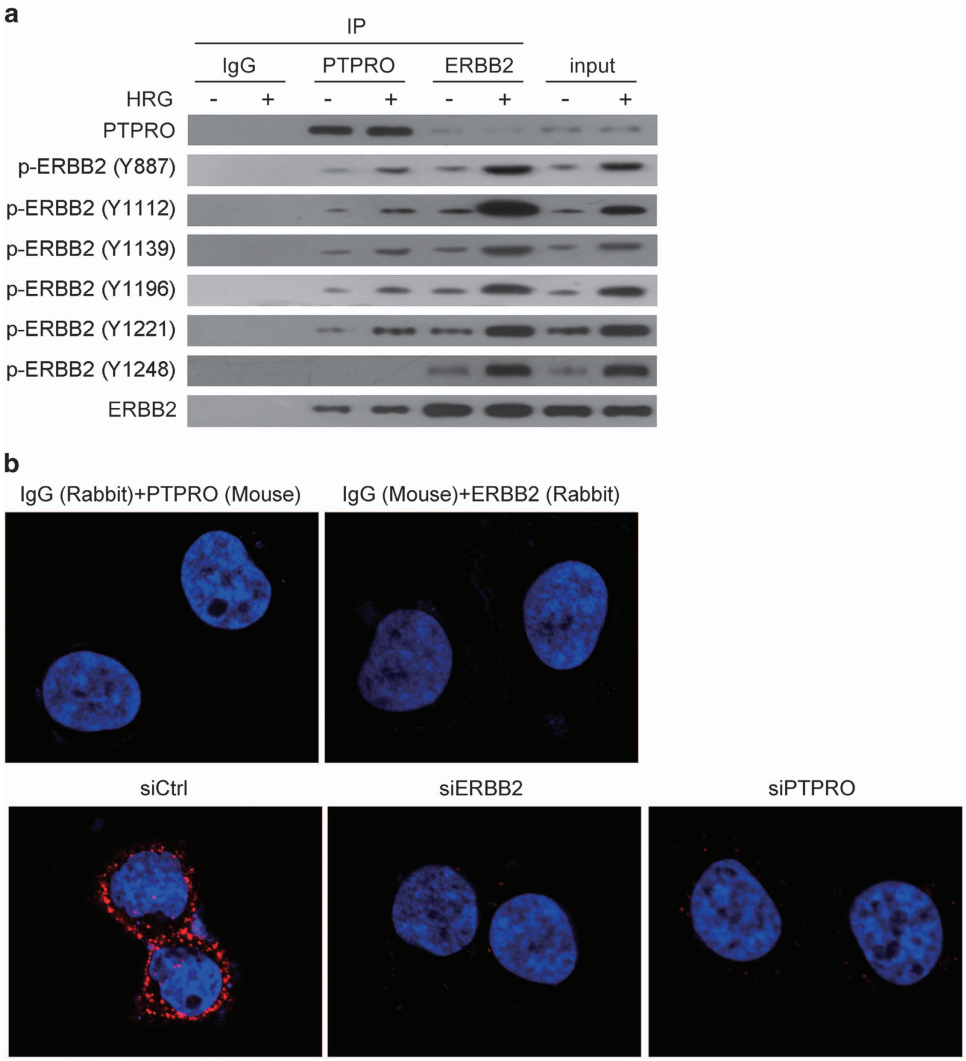


**Figure 2.** Interaction of PTPRO with ERBB2 in SKBR3 cells. (**a**) Co-immunoprecipitation showed interaction between PTPRO and ERBB2. SKBR3 cells were incubated with or without heregulin (HRG). Immunoprecipitation (IP) was performed using either anti-PTPRO or anti-ERBB2 antibodies. Immunoblots of immunoprecipitates were showed with the antigens as labeled to the left. (**b**) Duolink *in situ* proximity ligation assay (PLA) in SKBR3 cells. The top two fluorescent micrographs showed the negative controls in which a non-specific immunoglobulins (IgG) replaced either the anti-PTPRO or anti-ERBB2 antibody. Using both anti-PTPRO and anti-ERBB2 antibodies, positive reactions (Red) were detected in cells transfected with scramble control small interfering RNA (siCtrl) while knocking down either ERBB2 or PTPRO with siERBB2 or siPTPRO, respectively, abolished the signals. These results were representative of three independent experiments.

To examine the requirement of PTPRO phosphatase activity in the growth of breast cancer cells, we mutated the catalytic site (CS) of PTPRO[23] and transfected this plasmid into two ERBB2-positive SKBR3 and BT474 cell lines, which have low PTPRO levels (Figures 4a and b). Transfection of wild-type *PTPRO* inhibited the proliferation and colony formation of SKBR3 and BT474 cells as compared with empty vector, whereas the CS mutation of PTPRO only partially attenuated its inhibitory activity on cell growth and colony formation (Figures 4c and d). Flow cytometry studies showed a remarkable increase in the percentage of cells in the G1 phase in PTPRO-expressing cells compared with cells transfected with empty vector (control) or the PTPRO-CS mutant (Figure 4e). Flow cytometry for Annexin-V-FITC and PI staining did not show obvious difference in apoptosis among these cells (Figure 4f). These findings suggested that the enhancement of cell proliferation and cell cycle induced by *PTPRO* deletion was mimicked by the loss of PTPRO phosphatase activity.

ERBB2-dependent oncogenic signaling was antagonized by PTPRO in breast cancer

We next investigated whether PTPRO could regulate ERBB2 phosphorylation and ERBB2-dependent signaling in genetic model, MEFs derived from mice and human cancer cells. Results from the immunoblotting and immunohistochemistry (IHC) studies revealed an increased ERK1/2 (p44/42) phosphorylation as well as AKT phosphorylation in *Ptpro*$^{-/-}$ mouse mammary tissues and tumors as compared with wild-type controls, indicating the *in vivo* effects of PTPRO on AKT/ERK signaling (Figures 5a and d and Supplementary Figures 2A and B). In the same line of evidence, *Ptpro* deletion enhanced *ERBB2* signaling and activation of downstream mitogen-activated proteinkinase and phosphatidylinositol 3-kinase/AKT signaling pathways in cultured MEFs overexpressing *ERBB2* as compared with wild-type control (Figures 5b and e). Conversely, PTPRO overexpression in SKBR3 and BT474 breast cancer cells was accompanied by reduced phospho-ERK and phospho-AKT signaling as compared with vector control (Figures 5c and f), whereas

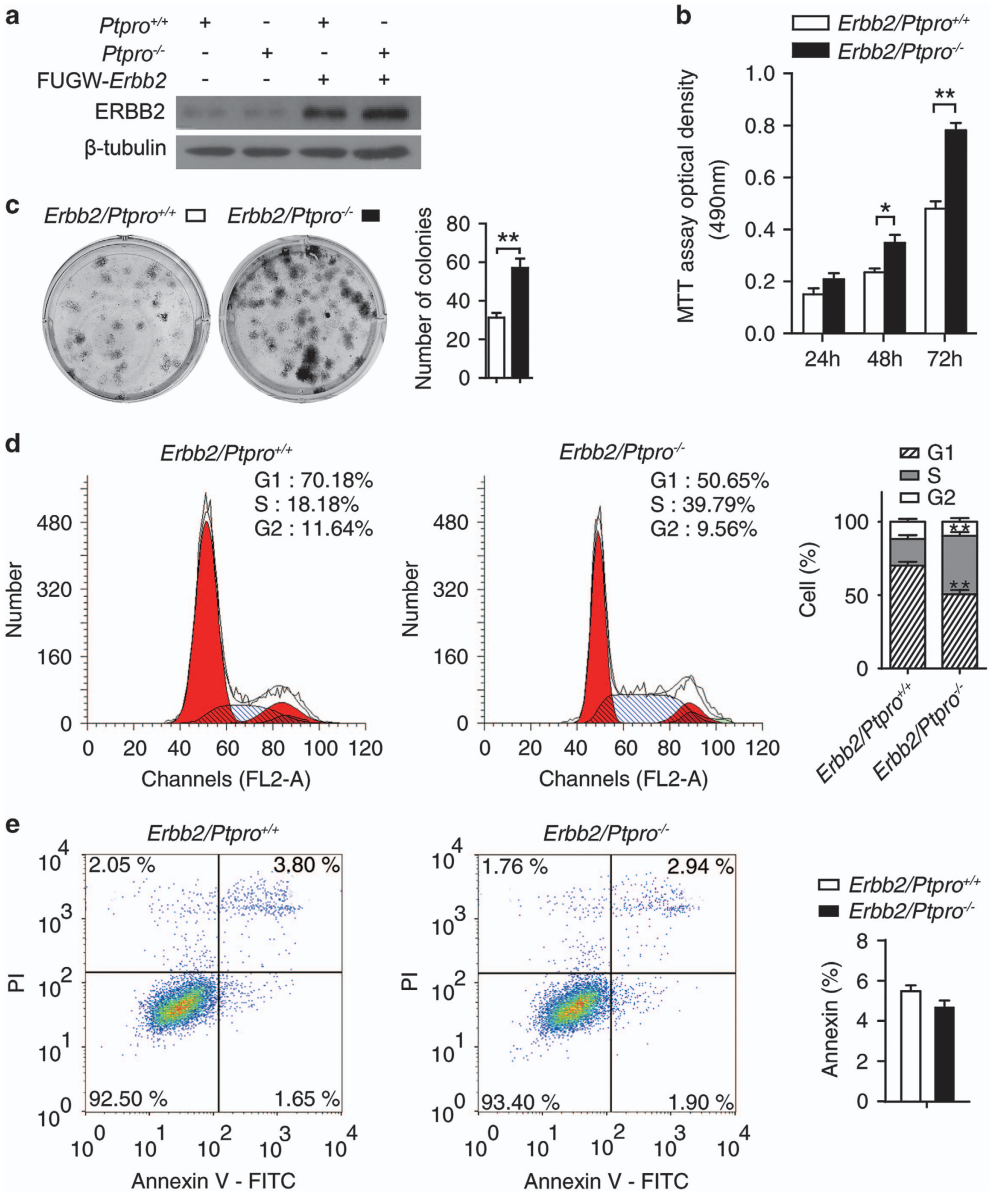


**Figure 3.** Effects of *Erbb2/Ptpro*$^{-/-}$MEFs on cell viability, cell proliferation and apoptosis. (**a**) Immunoblotting of two genotypic MEFs derived from littermates, which were stably transfected with FUGW-*Erbb2* vector or control vector. (**b**) *Erbb2/Ptpro*$^{+/+}$ MEFs and *Erbb2/Ptpro*$^{-/-}$ MEFs were inoculated in 96 wells for 24, 48 and 72 h, cell viability was measured by MTT assay. (**c**) *Erbb2/Ptpro*$^{+/+}$ MEFs and *Erbb2/Ptpro*$^{-/-}$ MEFs cells were seeded in a six-well plate and incubated for 2 weeks to allow colony formation (left). Quantitative determination of colony numbers (right). (**d**) Cell cycle analysis by flow cytometry in *Erbb2/Ptpro*$^{+/+}$ MEFs and *Erbb2/Ptpro*$^{-/-}$ MEFs. The bar graphs show the relative quantity of G1, G2 and S in the *Erbb2/Ptpro*$^{+/+}$ MEFs compared with the *Erbb2/Ptpro*$^{-/-}$ MEFs. (**e**) Apoptosis was determined by flow cytometry following Annexin-V-FITC and PI dual labeling. Samples shown are representative of three independent experiments. Error bars indicate s.e.m. $^{*}P < 0.05$, $^{**}P < 0.01$ by Student's *t*-test.

expression of PTPRO CS-mutant in SKBR3 cells did not impact the activation status of ERK and AKT (Figures 5c and f). Therefore, PTPRO phosphatase activity was required for its impact on ERBB2-AKT-ERK signaling.

In accordance with above findings, correlation analysis of clinical specimen of TMA demonstrated an inverse relationship between PTPRO and the phospho-ERBB2/ERBB2 ratio, phospho-ERK and phospho-AKT levels (PTPRO and phospho-ERBB2/ERBB2 ratio: $P < 0.001$; PTPRO and phospho-ERK: $P < 0.001$; PTPRO and phospho-AKT: $P < 0.001$; Figures 6a and b). Gene set enrichment analysis of published human breast cancer expression profiles[27] revealed that *PTPRO* expression was associated with reduced AKT and ERK signaling gene signatures in ERBB2-positive patients (Figure 6c). Together, these results suggested that PTPRO was an important modulator for ERBB2–AKT–ERK axis both in experimental and clinically relevant settings.

Since Y1248 is an autophosphorylation site,[28] Y1248-phosphorylated ERBB2 might increase as total ERBB2 increases. If the increase in phospho-Y1248 was merely due to increase in total ERBB2, then the ratio of phospho-ERBB2 to total ERBB2 should remain similar. We generated two stable PTPRO-knockdown cells in PTPRO-high ZR75-1 cell line, named ZR75-1-shPTPRO #1 and ZR75-1-shPTPRO #2. Immunoblotting showed that both ZR75-1-shPTPRO #1 and ZR75-1-shPTPRO #2 cells had increased phosphorylation of ERBB2 at Y1248 as compared with ZR75-1-shCtrl both in the basal state and with heregulin

stimulation. Importantly, the ratio of phospho-ERBB2 to total ERBB2 noticeably changed upon knockdown of PTPRO, especially when stimulated with heregulin (Supplementary Figure 3). These experiments suggested that loss of PTPRO-mediated dephosphorylation was the main cause of increase in phosphorylation at Y1248.

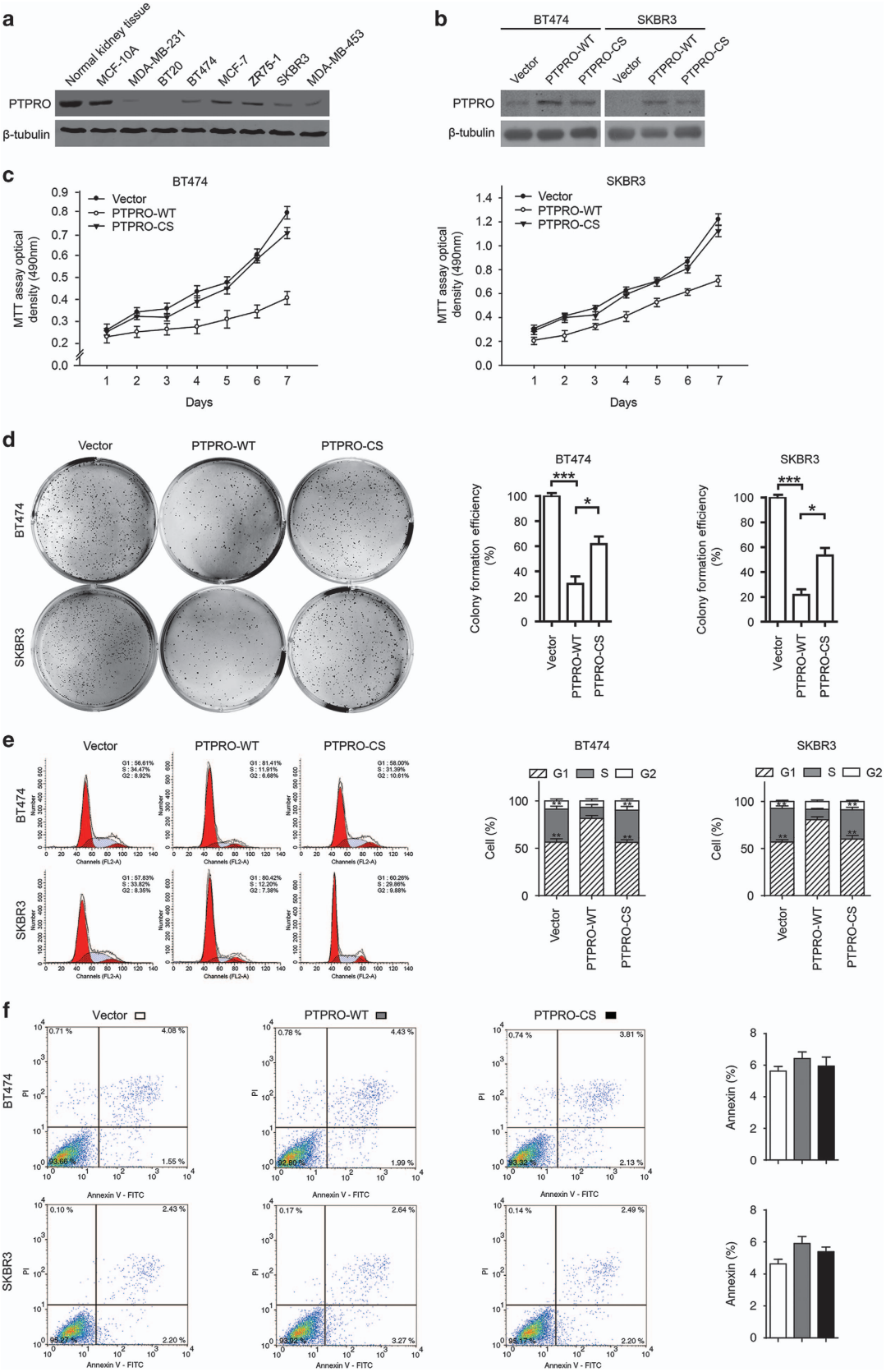

### PTPRO phosphatase activity was required for the endosomal internalization of ERBB2

Given that phosphatases can regulate RTKs at multiple levels through complex mechanisms,[29,30] we thus next investigated whether PTPRO phosphatase activity could control ERBB2 subcellular compartmentalization and internalization and thereby repressed ERBB2 oncogenic function. Flow cytometry assay showed that cell surface ERBB2 was decreased in PTPRO-overexpressing cells, whereas the amount of the cell surface ERBB2 was not obviously altered in CS mutation cells as compared with empty vector-transfected cells (Figure 7a). These results suggested that the internalization and trafficking of ERBB2 might be controlled by PTPRO phosphatase activity to repress ERBB2 signaling.

Internalization and degradation are known mechanisms for many RTKs' downregulation.[31] However, little is known for the role of dephosphorylation on the internalization of ERBB2.[9,11,16,17] To determine whether the observed PTPRO-mediated downregulation of ERBB2 might result from accelerated protein degradation, SKBR3 cells were treated for 0–24 h with the translation inhibitor cycloheximide to block *de novo* protein synthesis. PTPRO overexpression remarkably accelerated degradation of ERBB2 (Figure 7b). The half-life of ERBB2 protein decreased to 10.2 h as opposed to 19.6 h in control cells. However, this ERBB2 degradation appeared not to involve proteolysis through the ubiquitin-proteasome system as a proteasome inhibitor MG132 did not attenuate the PTPRO-induced degradation of ERBB2 (Figure 7b). In contrast, a lysosome inhibitor chloroquine abolished ERBB2 degradation in the presence of PTPRO overexpression (Figure 7b), suggesting that the acceleration of ERBB2 degradation by PTPRO was primarily through lysosomal degradation. In corroboration with this evidence, confocal immunofluorescence microscopy demonstrated that the accumulation of ERBB2 increased in endosomes (as shown by co-localization with EEA1) in PTPRO-overexpressing SKBR3 cells (Figure 7c, left panels), whereas CS mutation did not increase such accumulation compared with empty vector control (Figure 7c, left panels). Further, increased ERBB2 was detectable in lysosomes (as shown by LAMP-1 co-localization) of PTPRO-overexpressing cells compared with empty vector or CS mutant cells (Figure 7c, right panels). These data suggested that PTPRO phosphatase activity controlled the endocytotic degradation, contributing to ERBB2 downregulation.

To further address whether phosphorylation of Y1248 was determinant for the lysosomal degradation of ERBB2, we used site-directed mutagenesis to generate dephosphorylated-Y1248-mimicking (that is, mutated to phenylalanine (Y1248F)) and phosphorylated-Y1248-mimicking (that is, mutated to glutamate (Y1248E)) mutants.[32] In an ERBB2-negative cell line with low endogenous PTPRO expression (MDA-MB-231), we co-transfected PTPRO-WT or PTPRO-CS with ERBB2-WT or mutants of Y1248, and examined the cellular distribution of ERBB2 Y1248 mutants (Supplementary Figure 4A). As analyzed with confocal immunofluorescence microscopy, dephosphorylation-mimicking mutant of ERBB2, Y1248F, showed co-localization with an endosomal marker (EEA1) and a lysosomal marker (LAMP-1), which was comparable to the results for cells transfected with ERBB2-WT and PTPRO-WT plasmids (Supplementary Figures 4B and C, left panels). Although the loss of phosphatase activity in PTPRO-CS mutant blocked the co-localization with endosomal and lysosomal markers, this had no effect on the dephosphorylation-mimicking mutant (Supplementary Figures 4B and C, right panels). In contrast, the phosphotyrosine-mimicking mutant (Y1248E) did not co-localize with either endosomes or lysosomes in the presence of ectopic expression of PTPRO-WT or PTPRO-CS (Supplementary Figures 4B and C). Together, these data demonstrated that the phosphorylation status of Y1248-regulated endosomal internalization and lysosomal degradation of ERBB2, and dephosphorylation of Y1248 was the mechanism by which PTPRO phosphatase activity regulated these changes in ERBB2.

### Therapeutic potentials of epigenetic reexpression of PTPRO for suppressing ERBB2-positive breast cancer

We and others have previously documented *PTPRO* hypermethylation in breast cancer.[24,33] However, the PTP-associated gene inactivation involved in tumorigenesis and tumor progression may be due to point mutation or deletion, in addition to promoter hypermethylation.[34,35] To test this, we examined the frequency of genomic mutation or deletion in the coding region of *PTPRO*.[36] We analyzed data from the cBioPortal for Cancer Genomics (http://cbioportal.org).[37] The incidence of genomic PTPRO mutation was 0.4% of 962 cases (TCGA), 0.2% of 482 cases (TCGA pub) and 1% of 100 cases (Sanger); the rates of PTPRO deletion were 0.6% of 962 cases (TCGA), 0.0% of 482 cases (TCGA pub) and 0.0% of 100 cases (Sanger; Supplementary Figure 5A), whereas *PTPRO* hypermethylation inversely associated with *PTPRO* mRNA expression (Supplementary Figure 5B). Given that exon 1 and promoter regions of *PTPRO* contain typical CpG islands (Figure 8a), we performed methylation-specific PCR using genomic DNA extracted from 37 breast cancer specimens and their respective adjacent non-tumor tissues. In all, 25 (67.6%) of 37 cancer specimens exhibited a complete or partial DNA methylation, whereas 12 (32.4%) of the 37 adjacent non-tumor tissues had partial methylation and no methylation in the remaining non-tumor samples (Supplementary Figure 6A). Furthermore, the *PTPRO* promoter was hypermethylated in seven breast cancer cell lines, but not in immortalized non-cancerous MCF-10A and normal human mammary tissues (Supplementary Figure 6B). We quantified the relative levels of promoter methylation and protein expression by measuring densitometry of the corresponding bands using software 'Quantity one'. Pearson's correlation analysis showed that there was an inverse linear relationships between promoter methylation and protein expression of PTPRO ($r = -0.965$; $P = 0.002$; Supplementary Figure 6C). These results suggested that promoter hypermethylation, instead of genomic mutation and deletion, was the primary mechanism responsible for repressed *PTPRO* expression.

We next investigated the therapeutic potential that reexpression of PTPRO by epigenetic modification could suppress ERBB2-positive breast cancer. The DNA methyltransferase inhibitor 5'-aza-2'-deoxycytidine (5-aza-dC) was used to block promoter

**Figure 4.** Effect of PTPRO overexpression on cell viability, cell proliferation and apoptosis in ERBB2-overexpressing cell lines. (**a**) Levels of PTPRO protein in 7 breast cancer cell lines examined by immunoblotting. Normal kidney and MCF-10A cells were positive references. (**b**) Immunoblotting of breast cancer cells transfected with PTPRO-WT vector and mutant PTPRO-CS vector. (**c**) *PTPRO*-expressing cells had lower growth rates than that in empty vector and CS mutation of *PTPRO* cells as indicated by MTT assay. (**d**) *PTPRO*-expressing cells had lower clone formation ability than that in empty vector and CS mutation of *PTPRO* cells. (**e**) A remarkable increase in percentage of cells in G1 phase in *PTPRO*-expressing cells compared with cells transfected with empty vector or *PTPRO*-CS mutant cells as assayed by flow cytometry (left). The bar graphs showed the percentage of cells in G1, G2 and S phase (right). (**f**) Flow cytometry for Annexin-V-FITC and PI staining did not show visible difference in apoptotic cell distribution among these cells. Samples shown are representative of three independent experiments. Error bars indicate s.e.m. $^{*}P < 0.05$, $^{**}P < 0.01$, $^{***}P < 0.001$ by Student's *t*-test.

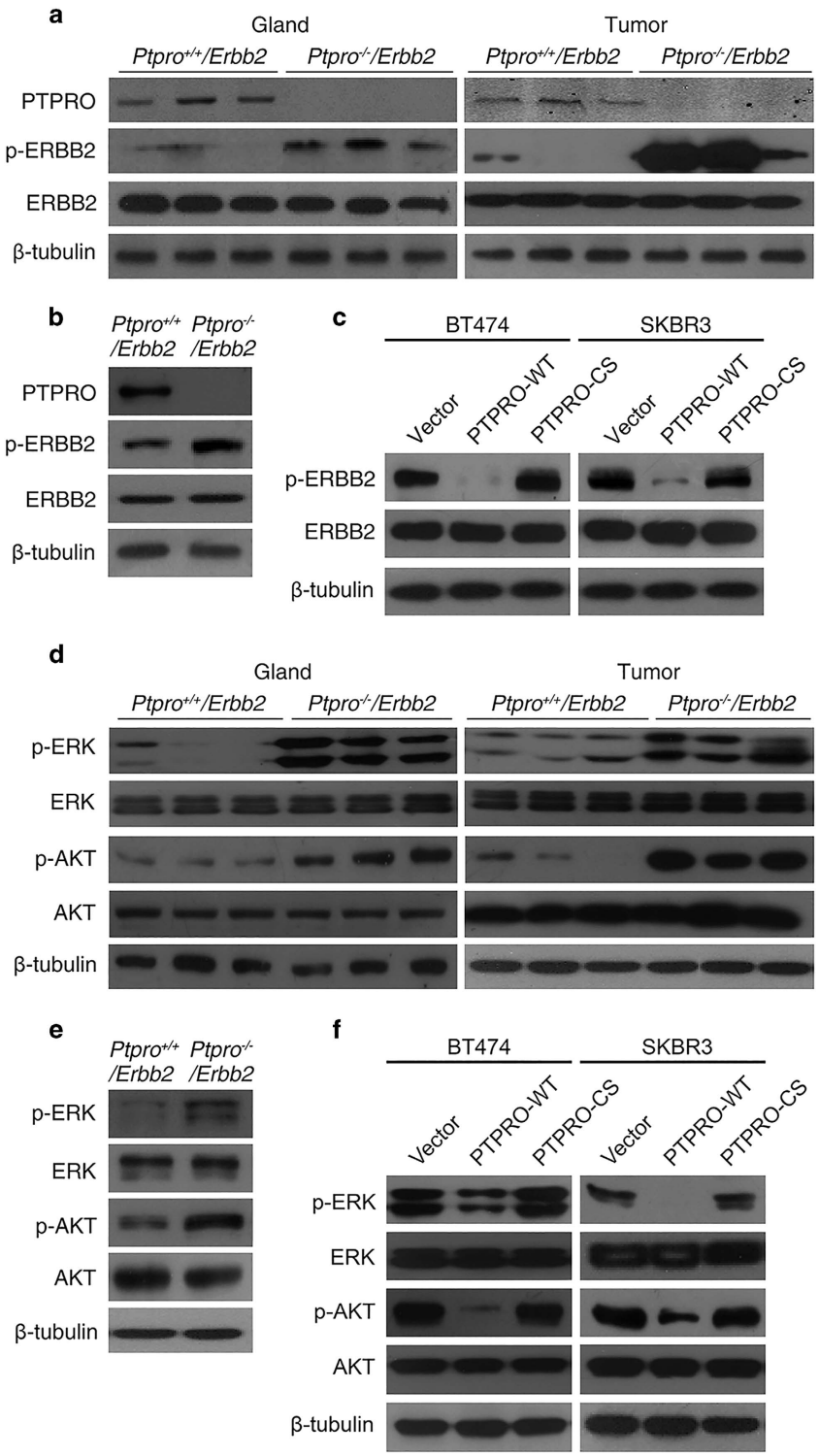


**Figure 5.** PTPRO modulates ERBB2 and downstream signaling through ERK/AKT pathways in breast cancer. (**a**) Immunoblots of mammary tissues from mice are shown with the antigens labeled on the left. ERBB2 phosphorylation was increased in mammary glands (4 months of age) and tumors (7 months of age) following *Ptpro* deletion in *Erbb2* transgenic mice compared with littermate controls. (**b**) ERBB2 phosphorylation was increased in *Erbb2/Ptpro*$^{-/-}$ MEFs compared with littermate controls. (**c**) ERBB2 phosphorylation was decreased in *PTPRO*-overexpressing breast cancer cells rather than in *PTPRO* mutant (CS) cells. (**d**) Immunoblots of mammary tissues from mice are shown with the antigens labeled on the left. ERK and AKT phosphorylation were increased in mammary glands (4 months of age) and tumors (7 months of age) following *Ptpro* deletion in *Erbb2* transgenic mice compared with littermate controls. (**e**) ERK and AKT phosphorylation were increased in *Erbb2/Ptpro*$^{-/-}$ MEFs compared with *Erbb2/Ptpro*$^{+/+}$ MEFs. (**f**) ERK and AKT phosphorylation were decreased in *PTPRO*-overexpressing breast cancer cells rather than in *PTPRO* mutant (CS) cells.

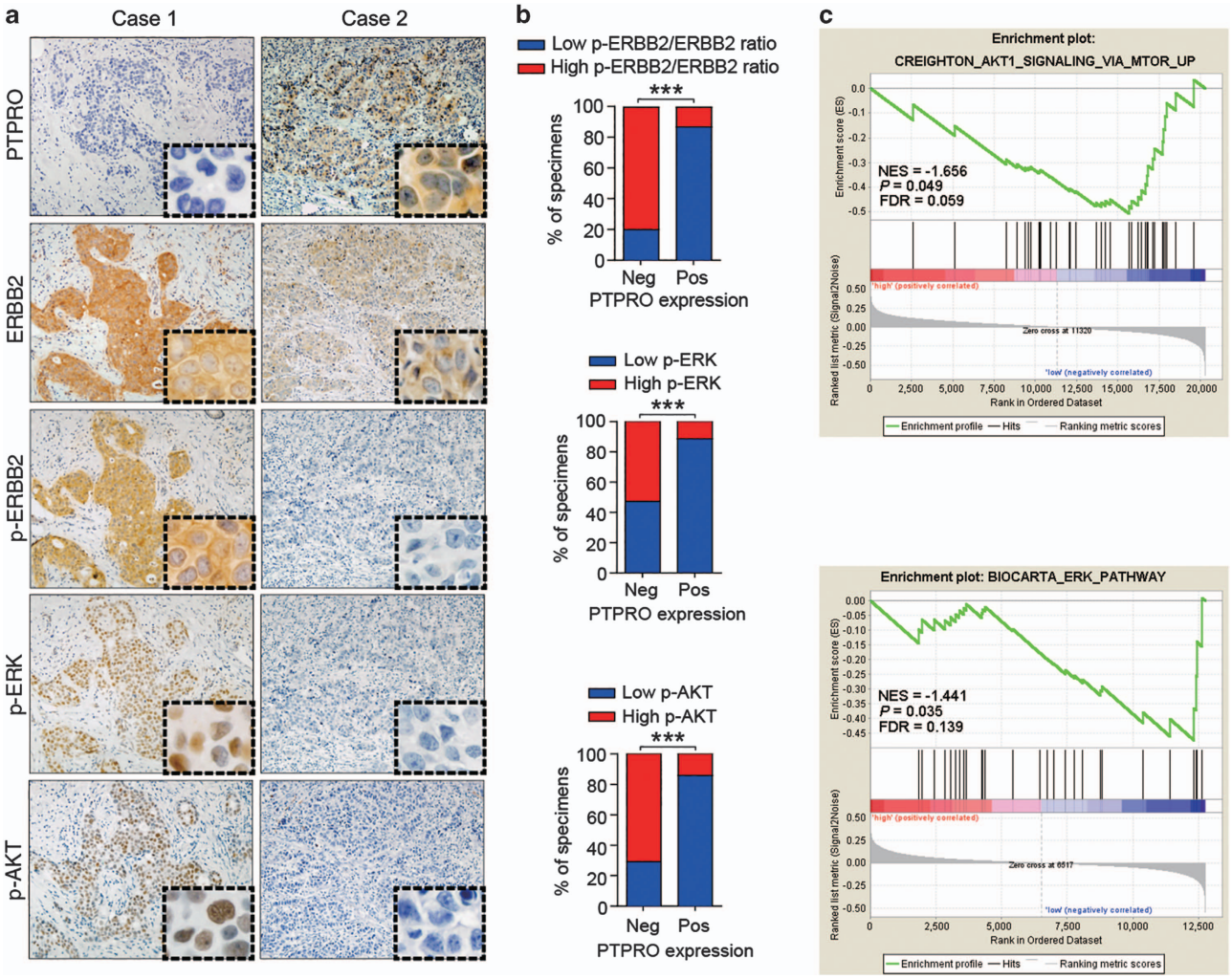


**Figure 6.** PTPRO expression correlated inversely with p-ERBB2, p-ERK and p-AKT in human breast cancer tissues. (**a**) Representative immunohistochemistry images for PTPRO, ERBB2, p-ERBB2, p-ERK and p-AKT in five serial sections of the same tumor from two primary human breast cancer specimens (magnification, the top panels: ×100; the bottom panels: ×400). (**b**) Percentage of samples showing low or high p-ERBB2/ERBB2 ratio, p-ERK and p-AKT expression (from top to bottom) relative to the levels of PTPRO in 180 cases of human breast cancer samples. (**c**) Gene set enrichment analysis showing inverse correlations between PTPRO expression and an AKT gene signature (CREIGHTON_AKT1_SIGNALING_VIA_MTOR_UP) and an ERK gene signature (BIOCARTA_ERK_PATHWAY) in a published cohort of breast cancer patients (GSE1456; the top tertile (48 cases) of *ERBB2* mRNA expression was assumed to be ERBB2-positive tumors). ***$P < 0.001$, Spearman's rank test. FDR, false-discovery rate *q* value; Neg., negative; NES, normalized enrichment score; Pos., positive.

methylation in BT474 and SKBR3 cells. 5-aza-dC treatment of cells decreased methylation, leading to reexpression of *PTPRO* (Figure 8b). Further, the demethylation treatment using 5-aza-dC effectively reduced the ERBB2-induced cell growth and transformation as evidenced by colony formation (Figures 8c and d), and knockdown of *PTPRO* expression using small interfering RNA (Figure 8c) diminished the effect of 5-aza-dC (Figure 8d). Thus, the effect of 5-aza-dC was at least in part mediated by reexpression of *PTPRO*. Moreover, ERBB2-dependent oncogenic signaling was blocked by demethylation treatment using 5-aza-dC (Figure 8e). Taken together, our data strongly argued that reexpression of *PTPRO* by treatment with 5-aza-dC could suppress ERBB2-positive breast cancer.

## DISCUSSION

Although prior epidemiologic, bioinformatics data and cellular studies are suggestive of a tumor-suppressor function for PTPRO in breast cancer,[24,25] definitive *in vivo* evidence has been lacking until this study. We used a genetic approach by breeding *Ptpro*-null mice with *MMTV-Erbb2* transgenic mice to characterize the role of *Ptpro* in breast tumorigenesis and cancer progression. Our *in vivo* results together with *in vitro* data, firmly establish *Ptpro* as a tumor-suppressor gene. To exclude the possibility that the noted phenotypes in *Ptpro* knockout mice could be due to effects of loss of *Ptpro* in non-breast tissue, we performed transplantation of mammary cells derived from mice. Data derived from tumor cell transplantation strongly argue that the accelerated tumor growth observed in $Ptpro^{-/-}$/*MMTV-Erbb2* mice is directly due to loss of *Ptpro* function within the breast cancer cells themselves.

It was unclear whether PTPRO repressed ERBB2-positive cancer by blocking the key oncogenic signaling downstream of ERBB2. Using non-malignant immortalized MCF-10A cells, a prior study showed that neither ERK nor AKT was activated by PTPRO downregulation.[25] However, we demonstrated that PTPRO regulated AKT and ERK activation in ERBB2-induced cancer cells using genetic mouse model, MEFs derived from transgenic mice, human cancer cells and patient specimens and bioinformatics data mining. The contrasting results from two studies may reflect the difference between non-malignant cells used in prior study and

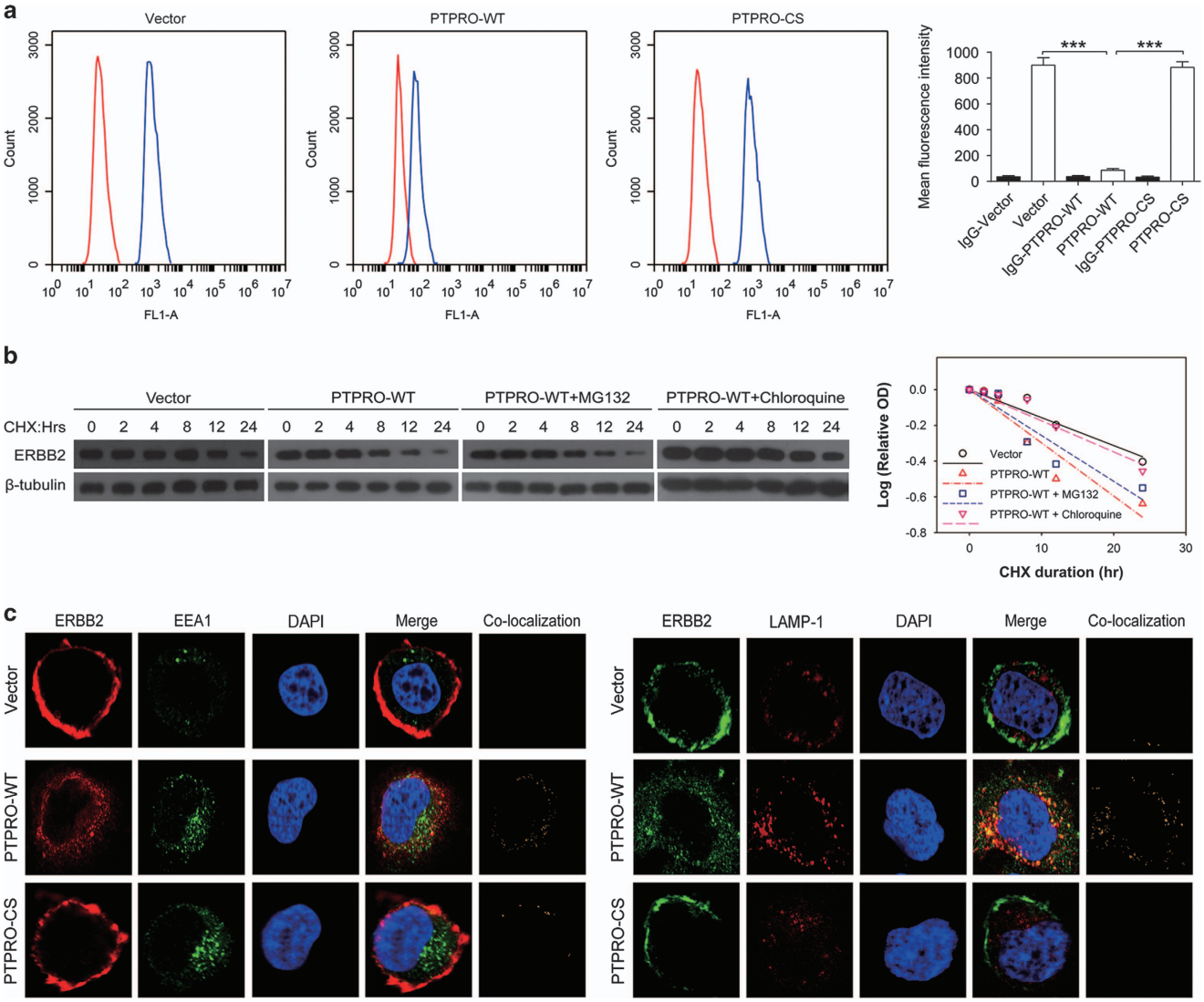


**Figure 7.** PTPRO reduced ERBB2 half-life. (**a**) Cell surface ERBB2 expression was reduced in *PTPRO*-expressing cells than that in empty vector and CS mutation of *PTPRO* cells as indicated by flow cytometry. Normal rabbit IgG as a control. Samples shown are representative of three independent experiments. Error bars indicate s.e.m. ***$P < 0.001$ by Student's *t*-test. (**b**) PTPRO-expressing cells were incubated with 20 μg/ml cycloheximide (CHX) for 0, 2, 4, 8, 12 or 24 h plus 10 μmol/l of MG132 or 100 μmol/l of chloroquine. ERBB2 and β-tubulin were detected by immunoblotting and measured by integrated optical density. Half-life (h): Vector: 19.6; PTPRO: 10.2; PTPRO+MG132: 11.8; PTPRO+Chloroquine: 18.0. The log relative optical density (OD) of a band is defined as the $\log_{10}$ (integrated OD of ERBB2/integrated OD of ERBB2 at time 0 h) - $\log_{10}$ (integrated OD of β-tubulin/integrated OD of β-tubulin at time 0 h). (**c**) PTPRO enhanced endocytosis of ERBB2. Representative confocal fluorescent micrographs are shown. The detected antigens were labeled at the top: ERBB2 and EEA1 (an early endosomes). Areas of co-localization were highlighted using Image J. (**d**) PTPRO-induced co-localization of ERBB2 and lysosomes. The experiment was similar to (**c**) except that LAMP-1 (a lysosomal maker) was examined instead of EEA1. DAPI, 4′-6-diamidino-2-phenylindole.

cancer cell systems used in our study. Our studies firmly establish a functional association between PTPRO phosphatase activity and ERBB2 oncogenic signaling using multiple experimental systems. We have verified that *PTPRO* deficiency promotes *ERBB2*-driven breast tumorigenesis via activating oncogenic signaling and the phosphatase catalytic site of PTPRO is required for its effect on ERBB2-AKT-ERK signaling. Our studies also highlight a new conceptual framework in which PTPRO downregulates tyrosine phosphorylation of multiple oncogenic pathways in breast carcinogenesis.

Several PTPs have been previously reported to either positively or negatively regulate ERBB2 tyrosine phosphorylation.[11–17] However, structural analysis of the tyrosine phosphatome showed that PTPRO is distinct in structure, catalytic activity and substrate recognition.[38] Although ERBB2 has been reported to be the substrate of PTPRO,[25] the specific tyrosine residue that is selectively catalyzed by PTPRO remains unknown. In this study, our co-immunoprecipitation experiment along with the results derived from *in vivo*, cultured cells and clinical specimen confirm that PTPRO dephosphorylates ERBB2 at Y1248. Among the multiple ERBB2 tyrosine phosphorylation sites, Y1248 has been documented to be biologically important and clinically significant. Y1248 has a role in cell differentiation as MUC4/SMC forms a complex with ERBB2, which leads to Y1248 phosphorylation[39] and translocation of ERBB2 to the apical surface of polarized epithelial cells.[40] In breast cancer, activated Y1248 ERBB2 was detected in 20% of patients,[41] and the expression of this phosphorylation site is highly specific for ERBB2 gene amplification.[42] Importantly, phosphorylation of Y1248 shows prognostic value; increased ERBB2 phosphorylation of Y1248 represents a lower 5-year

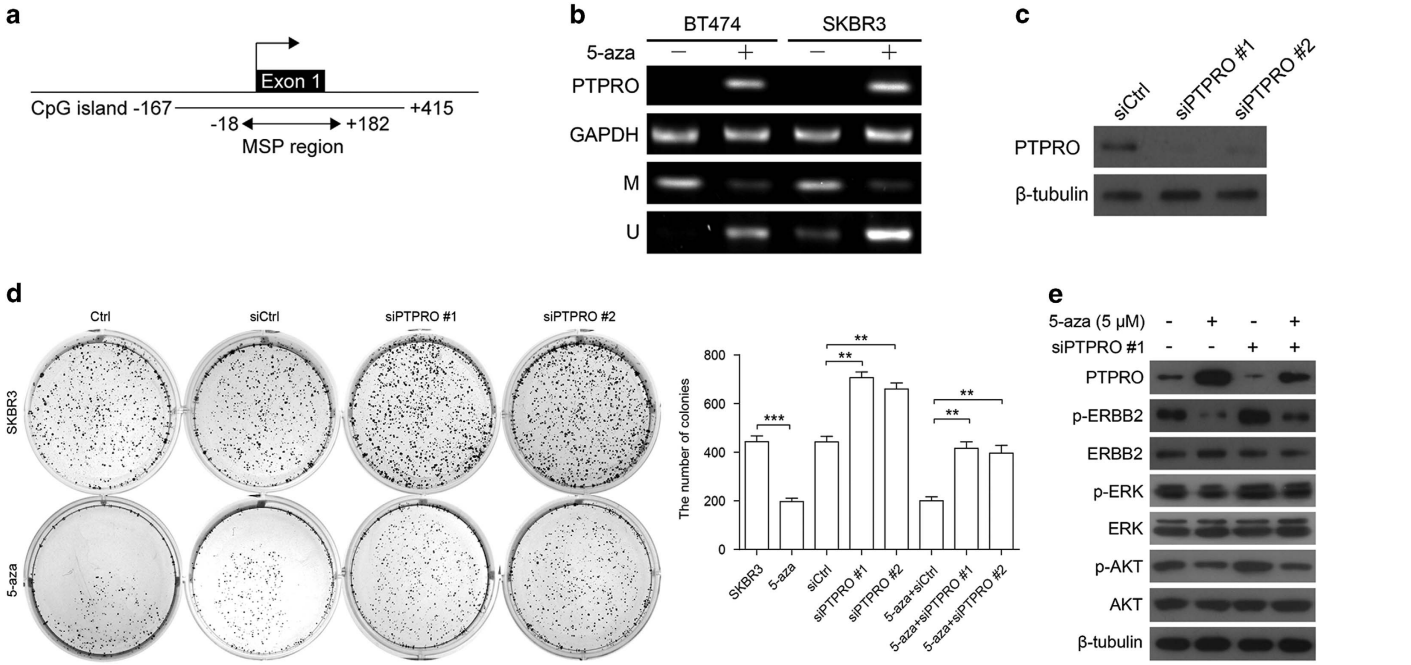


**Figure 8.** 5′-Aza-2′-deoxycytidine (5-aza-dC) reduced cell growth that was due to low *PTPRO* expression. (**a**) The methylation-specific PCR (MSP) region of the *PTPRO* gene CpG island. (**b**) Restored expression of *PTPRO* by treatment of 5-aza-dC. Expression and methylation analysis of *PTPRO* in BT474 and SKBR3 cell lines incubated with or without 5-aza-dC. GAPDH was used as an internal loading control. M, methylated; U, unmethylated. (**c**) Immunoblotting revealed that *PTPRO* was efficiently knocked down by the treatment of siPTPRO #1 or siPTPRO #2. (**d**) siPTPRO #1 or siPTPRO #2 cells were treated with and without 5 μM 5-aza-dC for 10 days to allow colony formation (left). Quantitative determination of colony numbers (right). (**e**) Combination of 5-aza-dC and siPTPRO treatment. SKBR3 cells were treated with siPTPRO #1 for 48 h before incubation with 5 μM 5-aza-dC. Cell lysates were immunoblotted with the labeled antibodies on the left. $^{**}P < 0.01$, $^{***}P < 0.001$ by Student's *t*-test.

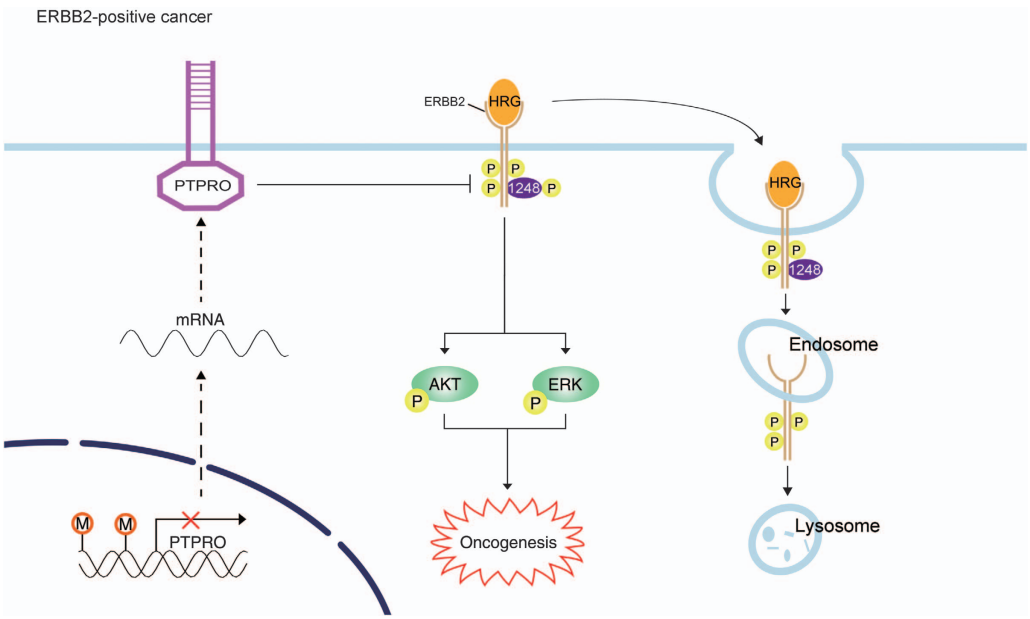


**Figure 9.** Schematic summary of the role of PTPRO in ERBB2-driven breast carcinogenesis: PTPRO is regulated epigenetically by methylation. PTPRO suppresses ERBB2 signaling through both tyrosine dephosphorylation of ERBB2 at Y1248 and endocytotic internalization and subsequent degradation.

disease-free survival rate than patients with low levels phosphorylation of Y1248,[43] and Y1248 phosphorylation is an independent predictors of progression-free survival.[41] Of note, Y1248 is known to activate mitogen-activated proteinkinase and mediate cell proliferation,[42,44,45] which supports our findings that PTPRO regulates ERBB2-induced ERK activation and cancer cell proliferation. We also used proximity ligation assay (Duolink) to provide the first evidence that PTPRO and ERBB2 directly bind each other on the cell membrane and in the cytoplasm.

Signaling of RTKs can be regulated at multiple levels. At the receptor level, the quantity of RTKs on the cell surface can be controlled by post-translational modification (for example,

dephosphorylation), endocytosis and then degradation via lysosomal or ubiquitin-proteasome system.[12,46] Nevertheless, protein degradation of ERBB2 is poorly understood.[16,47] In this study, we have found that PTPRO regulates the internalization of ERBB2 via endocytosis and subsequent lysosomal degradation. Further, we have revealed that PTPRO catalytic activity is required for the internalization. Thus, PTPRO phosphatase activity is critical for both dephosphorylation and internalization, which is eventually responsible for PTPRO-mediated ERBB2 downregulation (Figure 9).

*PTPRO* is located on chromosomal region 12p12.3, which is characterized by loss of heterozygosity in different types of cancers.[20–23] In contrast to several other PTPs,[34,48,49] we have found that *PTPRO* mutation and deletion are rare in human breast cancer. Given our previous result of high prevalence of *PTPRO* promoter hypermethylation in breast cancer,[24] we conclude that promoter hypermethylation is the major mechanism for *PTPRO* gene silencing in breast cancer.

Promoter hypermethylation provides a promising molecular target for epigenetic therapy of cancer. As such, we have found that reexpression of PTPRO by treatment with 5-aza-dC can effectively blocked ERBB2-dependent oncogenic signaling as well as tumor growth in cancers with PTPRO silencing. Based on the findings in this study, it is tempting to speculate that reactivation of *PTPRO* expression through epigenetic modification may be further explored in clinical settings either alone or in combination with targeted therapy. Because loss of *PTPRO* expression has also been reported in hepatomas,[21,50] colon cancer[22,51] and lung cancer,[23] we believe that our molecular insights are likely to be of a broad significance in cancer at-large.

In summary, these studies have established the role of PTPRO as a tumor suppressor in breast cancer *in vivo*. The model of epigenetic control of PTPRO-mediated ERBB2-AKT-ERK pathway largely reflects the clinical conditions in breast cancer. PTPRO phosphatase activity is required for dephosphorylation, endocytosis and lysosomal degradation of ERBB2, leading to the downregulation of its downstream signaling. The discovered importance of PTPRO in this study will shed light on how to target ERBB2-driven cancers by either selecting the right patients for personalized cancer therapy or designing further therapeutic strategies or both of such approaches.

## MATERIALS AND METHODS

### Mice

The *Ptpro*$^{-/-}$mice, gifts from Dr Bixby, University of Miami, and FVB/N mice carrying the *Erbb2* gene (*MMTV-Erbb2*) were obtained from Jackson Laboratories. All mice were maintained and bred at the Animal Center of Shantou University Medical College. *Ptpro*$^{-/-}$ mice were bred with wild-type FVB/N mice for 10 generation to obtain *Ptpro*$^{-/-}$mice with 99.90% FVB/N background, which took about 2 years, and their female offspring were paired with male *MMTV/Erbb2* transgenic mice with a FVB strain background. Age-matched *Ptpro*$^{+/+}$*/MMTV-Erbb2* and *Ptpro*$^{-/-}$*/MMTV-Erbb2* virgin mice with 99.95% FVB/N genetic background (11 generation backcross to FVB/N strain) were used for further experiments. Littermates with both genotypes were used in the same phenotypic alterations whenever it was possible. Their genotypes were identified by PCR analyses of tail DNA samples, as described previously.[52,53] The primers of mice genotypes analysis are listed in Supplementary Table 2. Animals were housed in pathogen-free conditions at the Animal Center of Shantou University Medical College in compliance with Institutional Animal Care and Use Committee regulations (SUMC2014-148). All animal experiments were performed according to protocols approved by the Animal Care and Use Committee of the Medical College of Shantou University.

### Patient specimens

Surgically treated female breast cancer patients ($n = 180$) with confirmed pathology of invasive ductal carcinoma were collected for preparation of tissue microarray (see Supplementary Information) for IHC and methylation-specific PCR. Breast cancer tissues were obtained from the patients when undergoing surgical treatment at the Department of Surgery, Cancer Hospital of Shantou University Medical College, during the period from 2010 to 2013. All patients received primary treatment by surgery followed by adjuvant radiotherapy, chemotherapy or hormone therapy. A total of 180 primary breast cancer patients contained all subtypes of breast cancer (that is, luminal A, luminal B, ERBB2-enriched and basal-like), including 60 ERBB2-positive patients. Clinical research protocols of this study were reviewed and approved by the Institutional Review Board and the Ethics Committee of Cancer Hospital of Shantou University Medical College (IRB serial number: # 04–070). Written informed consents were obtained from patients in accordance with principles expressed in the Declaration of Helsinki.

## CONFLICT OF INTEREST

The authors declare no conflict of interest.

## ACKNOWLEDGEMENTS

This work was supported in part by National Natural Science Foundation of China NSFC (81071736, 30973508 and 81572876 to HZ and 31271495 to HS), the funding for Collaborative and Creative Center, Molecular Diagnosis and Personalized Medicine, Shantou University, Guangdong Province, and the funding from the Department of Education, Guangdong Government under the Top-tier University Development Scheme for Research and Control of Infectious Diseases. We thank Dr Stanley Lin for the careful reading the manuscript.

## REFERENCES

1 Parker JS, Mullins M, Cheang MC, Leung S, Voduc D, Vickery T *et al.* Supervised risk predictor of breast cancer based on intrinsic subtypes. *J Clin Oncol* 2009; **27**: 1160–1167.
2 Gradishar WJ. Emerging approaches for treating HER2-positive metastatic breast cancer beyond trastuzumab. *Ann Oncol* 2013; **24**: 2492–2500.
3 Arteaga CL, Sliwkowski MX, Osborne CK, Perez EA, Puglisi F, Gianni L. Treatment of HER2-positive breast cancer: current status and future perspectives. *Nat Rev Clin Oncol* 2012; **9**: 16–32.
4 Stern HM. Improving treatment of HER2-positive cancers: opportunities and challenges. *Sci Transl Med* 2012; **4**: 127rv122.
5 Alimandi M, Romano A, Curia MC, Muraro R, Fedi P, Aaronson SA *et al.* Cooperative signaling of ErbB3 and ErbB2 in neoplastic transformation and human mammary carcinomas. *Oncogene* 1995; **10**: 1813–1821.
6 Jones RB, Gordus A, Krall JA, MacBeath G. A quantitative protein interaction network for the ErbB receptors using protein microarrays. *Nature* 2006; **439**: 168–174.
7 Hynes NE, Lane HA. ERBB receptors and cancer: the complexity of targeted inhibitors. *Nat Rev Cancer* 2005; **5**: 341–354.
8 Bard-Chapeau EA, Li S, Ding J, Zhang SS, Zhu HH, Princen F *et al.* Ptpn11/Shp2 acts as a tumor suppressor in hepatocellular carcinogenesis. *Cancer Cell* 2011; **19**: 629–639.
9 Sun T, Aceto N, Meerbrey KL, Kessler JD, Zhou C, Migliaccio I *et al.* Activation of multiple proto-oncogenic tyrosine kinases in breast cancer via loss of the PTPN12 phosphatase. *Cell* 2011; **144**: 703–718.
10 Aceto N, Sausgruber N, Brinkhaus H, Gaidatzis D, Martiny-Baron G, Mazzarol G *et al.* Tyrosine phosphatase SHP2 promotes breast cancer progression and maintains tumor-initiating cells via activation of key transcription factors and a positive feedback signaling loop. *Nat Med* 2012; **18**: 529–537.
11 Gensler M, Buschbeck M, Ullrich A. Negative regulation of HER2 signaling by the PEST-type protein-tyrosine phosphatase BDP1. *J Biol Chem* 2004; **279**: 12110–12116.
12 Wang HM, Xu YF, Ning SL, Yang DX, Li Y, Du YJ *et al.* The catalytic region and PEST domain of PTPN18 distinctly regulate the HER2 phosphorylation and ubiquitination barcodes. *Cell Res* 2014; **24**: 1067–1090.
13 Arias-Romero LE, Saha S, Villamar-Cruz O, Yip SC, Ethier SP, Zhang ZY *et al.* Activation of Src by protein tyrosine phosphatase 1B Is required for ErbB2 transformation of human breast epithelial cells. *Cancer Res* 2009; **69**: 4582–4588.
14 Julien SG, Dube N, Read M, Penney J, Paquet M, Han Y *et al.* Protein tyrosine phosphatase 1B deficiency or inhibition delays ErbB2-induced mammary tumorigenesis and protects from lung metastasis. *Nat Genet* 2007; **39**: 338–346.
15 Meyer DS, Aceto N, Sausgruber N, Brinkhaus H, Muller U, Pallen CJ *et al.* Tyrosine phosphatase PTPalpha contributes to HER2-evoked breast tumor initiation and maintenance. *Oncogene* 2014; **33**: 398–402.

16 Yuan T, Wang Y, Zhao ZJ, Gu H. Protein-tyrosine phosphatase PTPN9 negatively regulates ErbB2 and epidermal growth factor receptor signaling in breast cancer cells. *J Biol Chem* 2010; **285**: 14861–14870.
17 Zhu JH, Chen R, Yi W, Cantin GT, Fearns C, Yang Y *et al.* Protein tyrosine phosphatase PTPN13 negatively regulates Her2/ErbB2 malignant signaling. *Oncogene* 2008; **27**: 2525–2531.
18 Chen B, Bixby JL. A novel substrate of receptor tyrosine phosphatase PTPRO is required for nerve growth factor-induced process outgrowth. *J Neurosci* 2005; **25**: 880–888.
19 Stepanek L, Sun QL, Wang J, Wang C, Bixby JL. CRYP-2/cPTPRO is a neurite inhibitory repulsive guidance cue for retinal neurons *in vitro*. *J Cell Biol* 2001; **154**: 867–878.
20 You YJ, Chen YP, Zheng XX, Meltzer SJ, Zhang H. Aberrant methylation of the PTPRO gene in peripheral blood as a potential biomarker in esophageal squamous cell carcinoma patients. *Cancer Lett* 2012; **315**: 138–144.
21 Motiwala T, Ghoshal K, Das A, Majumder S, Weichenhan D, Wu YZ *et al.* Suppression of the protein tyrosine phosphatase receptor type O gene (PTPRO) by methylation in hepatocellular carcinomas. *Oncogene* 2003; **22**: 6319–6331.
22 Mori Y, Yin J, Sato F, Sterian A, Simms LA, Selaru FM *et al.* Identification of genes uniquely involved in frequent microsatellite instability colon carcinogenesis by expression profiling combined with epigenetic scanning. *Cancer Res* 2004; **64**: 2434–2438.
23 Motiwala T, Kutay H, Ghoshal K, Bai S, Seimiya H, Tsuruo T *et al.* Protein tyrosine phosphatase receptor-type O (PTPRO) exhibits characteristics of a candidate tumor suppressor in human lung cancer. *Proc Natl Acad Sci USA* 2004; **101**: 13844–13849.
24 Huang YT, Li FF, Ke C, Li Z, Li ZT, Zou XF *et al.* PTPRO promoter methylation is predictive of poorer outcome for HER2-positive breast cancer: indication for personalized therapy. *J Transl Med* 2013; **11**: 245.
25 Yu M, Lin G, Arshadi N, Kalatskaya I, Xue B, Haider S *et al.* Expression profiling during mammary epithelial cell three-dimensional morphogenesis identifies PTPRO as a novel regulator of morphogenesis and ErbB2-mediated transformation. *Mol Cell Biol* 2012; **32**: 3913–3924.
26 Weibrecht I, Leuchowius KJ, Clausson CM, Conze T, Jarvius M, Howell WM *et al.* Proximity ligation assays: a recent addition to the proteomics toolbox. *Expert Rev Proteomics* 2010; **7**: 401–409.
27 Pawitan Y, Bjohle J, Amler L, Borg AL, Egyhazi S, Hall P *et al.* Gene expression profiling spares early breast cancer patients from adjuvant therapy: derived and validated in two population-based cohorts. *Breast Cancer Res* 2005; **7**: R953–R964.
28 Chaturvedi P, Singh AP, Chakraborty S, Chauhan SC, Bafna S, Meza JL *et al.* MUC4 mucin interacts with and stabilizes the HER2 oncoprotein in human pancreatic cancer cells. *Cancer Res* 2008; **68**: 2065–2070.
29 Monast CS, Furcht CM, Lazzara MJ. Computational analysis of the regulation of EGFR by protein tyrosine phosphatases. *Biophys J* 2012; **102**: 2012–2021.
30 Schneeberger VE, Ren Y, Luetteke N, Huang Q, Chen L, Lawrence HR *et al.* Inhibition of Shp2 suppresses mutant EGFR-induced lung tumors in transgenic mouse model of lung adenocarcinoma. *Oncotarget* 2015; **6**: 6191–6202.
31 Miaczynska M. Effects of membrane trafficking on signaling by receptor tyrosine kinases. *Cold Spring Harb Perspect Biol* 2013; **5**: a009035.
32 Anthis NJ, Haling JR, Oxley CL, Memo M, Wegener KL, Lim CJ *et al.* Beta integrin tyrosine phosphorylation is a conserved mechanism for regulating talin-induced integrin activation. *J Biol Chem* 2009; **284**: 36700–36710.
33 Ramaswamy B, Majumder S, Roy S, Ghoshal K, Kutay H, Datta J *et al.* Estrogen-mediated suppression of the gene encoding protein tyrosine phosphatase PTPRO in human breast cancer: mechanism and role in tamoxifen sensitivity. *Mol Endocrinol* 2009; **23**: 176–187.
34 Zhao S, Sedwick D, Wang Z. Genetic alterations of protein tyrosine phosphatases in human cancers. *Oncogene* 2015; **34**: 3885–3894.
35 Veeriah S, Brennan C, Meng S, Singh B, Fagin JA, Solit DB *et al.* The tyrosine phosphatase PTPRD is a tumor suppressor that is frequently inactivated and mutated in glioblastoma and other human cancers. *Proc Natl Acad Sci USA* 2009; **106**: 9435–9440.
36 Cancer Genome Atlas N, Comprehensive molecular portraits of human breast tumours. *Nature* 2012; **490**: 61–70.
37 Gao J, Aksoy BA, Dogrusoz U, Dresdner G, Gross B, Sumer SO *et al.* Integrative analysis of complex cancer genomics and clinical profiles using the cBioPortal. *Sci Signal* 2013; **6**: pl1.
38 Barr AJ, Ugochukwu E, Lee WH, King ON, Filippakopoulos P, Alfano I *et al.* Large-scale structural analysis of the classical human protein tyrosine phosphatome. *Cell* 2009; **136**: 352–363.
39 Ramsauer VP, Pino V, Farooq A, Carothers Carraway CA, Salas PJ, Carraway KL. Muc4-ErbB2 complex formation and signaling in polarized CACO-2 epithelial cells indicate that Muc4 acts as an unorthodox ligand for ErbB2. *Mol Biol Cell* 2006; **17**: 2931–2941.
40 Ramsauer VP, Carraway CA, Salas PJ, Carraway KL. Muc4/sialomucin complex, the intramembrane ErbB2 ligand, translocates ErbB2 to the apical surface in polarized epithelial cells. *J Biol Chem* 2003; **278**: 30142–30147.
41 Hudelist G, Kostler WJ, Czerwenka K, Kubista E, Attems J, Muller R *et al.* Her-2/neu and EGFR tyrosine kinase activation predict the efficacy of trastuzumab-based therapy in patients with metastatic breast cancer. *Int J Cancer* 2006; **118**: 1126–1134.
42 Taniyama K, Ishida K, Toda T, Motoshita J, Kuraoka K, Saito A *et al.* Tyrosine1248-phosphorylated HER2 expression and HER2 gene amplification in female invasive ductal carcinomas. *Breast Cancer* 2008; **15**: 231–240.
43 Hayashi N, Iwamoto T, Gonzalez-Angulo AM, Ferrer-Lozano J, Lluch A, Niikura N *et al.* Prognostic impact of phosphorylated HER-2 in HER-2+ primary breast cancer. *Oncologist* 2011; **16**: 956–965.
44 Dankort D, Jeyabalan N, Jones N, Dumont DJ, Muller WJ. Multiple ErbB-2/Neu phosphorylation sites mediate transformation through distinct effector proteins. *J Biol Chem* 2001; **276**: 38921–38928.
45 Cicenas J, Urban P, Kung W, Vuaroqueaux V, Labuhn M, Wight E *et al.* Phosphorylation of tyrosine 1248-ERBB2 measured by chemiluminescence-linked immunoassay is an independent predictor of poor prognosis in primary breast cancer patients. *Eur J Cancer* 2006; **42**: 636–645.
46 Marmor MD, Yarden Y. Role of protein ubiquitylation in regulating endocytosis of receptor tyrosine kinases. *Oncogene* 2004; **23**: 2057–2070.
47 Roepstorff K, Grovdal L, Grandal M, Lerdrup M, van Deurs B. Endocytic down-regulation of ErbB receptors: mechanisms and relevance in cancer. *Histochem Cell Biol* 2008; **129**: 563–578.
48 Wang Z, Shen D, Parsons DW, Bardelli A, Sager J, Szabo S *et al.* Mutational analysis of the tyrosine phosphatome in colorectal cancers. *Science* 2004; **304**: 1164–1166.
49 Lui VW, Peyser ND, Ng PK, Hritz J, Zeng Y, Lu Y *et al.* Frequent mutation of receptor protein tyrosine phosphatases provides a mechanism for STAT3 hyper-activation in head and neck cancer. *Proc Natl Acad Sci USA* 2014; **111**: 1114–1119.
50 Hou J, Xu J, Jiang R, Wang Y, Chen C, Deng L *et al.* Estrogen-sensitive PTPRO expression represses hepatocellular carcinoma progression by control of STAT3. *Hepatology* 2013; **57**: 678–688.
51 Asbagh LA, Vazquez I, Vecchione L, Budinska E, De Vriendt V, Baietti MF *et al.* The tyrosine phosphatase PTPRO sensitizes colon cancer cells to anti-EGFR therapy through activation of SRC-mediated EGFR signaling. *Oncotarget* 2014; **5**: 10070–10083.
52 Zhang H, Kuang SQ, Liao L, Zhou S, Xu J. Haploid inactivation of the amplified-in-breast cancer 3 coactivator reduces the inhibitory effect of peroxisome proliferator-activated receptor gamma and retinoid X receptor on cell proliferation and accelerates polyoma middle-T antigen-induced mammary tumorigenesis in mice. *Cancer Res* 2004; **64**: 7169–7177.
53 Zhang H, Singh RR, Talukder AH, Kumar R. Metastatic tumor antigen 3 is a direct corepressor of the Wnt4 pathway. *Genes Dev* 2006; **20**: 2943–2948.



Supplementary Information accompanies this paper on the Oncogene website (http://www.nature.com/onc)